PAPER • OPEN ACCESS

Structural properties controlled magnetisation of Ni/Al multilayers sputtered on flexible polymer substrate: Impact of Ni deposition rates

To cite this article: Nadir Kaplan *et al* 2024 *Phys. Scr.* **99** 065975

IOP Publishing Phys. Scr. 99 (2024) 065975 https://doi.org/10.1088/1402-4896/ad48c7

Physica Scripta

CrossMark

OPEN ACCESS

RECEIVED
25 January 2024

REVISED
16 April 2024

ACCEPTED FOR PUBLICATION
8 May 2024

PUBLISHED
17 May 2024

PAPER

Structural properties controlled magnetisation of Ni/Al multilayers sputtered on flexible polymer substrate: Impact of Ni deposition rates

Nadir Kaplan[1], **Ali Karpuz**[2] and **Hakan Köçkar**[1,*]

[1] Department of Physics, Science & Literature Faculty, Balikesir University, Balikesir, Turkey
[2] Department of Physics, Kamil Ozdag Science Faculty, Karamanoglu Mehmetbey University, Karaman, Turkey
[*] Author to whom any correspondence should be addressed.

E-mail: nadirkaplan@baun.edu.tr, alikarpuz@kmu.edu.tr and hkockar@balikesir.edu.tr

Keywords: Ni/Al multilayer thin films, Ni deposition rate, structural properties, magnetisation, sputtering technique

Abstract

The goal of this work is to determine how the rate of Ni deposition rates affect the structural characteristics that regulate the magnetization of Ni/Al multilayer thin films sputtered on flexible acrylic acetate polymer substrates. The films with a 5[Ni(20 nm)/Al(10 nm)] structure were gradually sputtered as different Ni deposition rates in the total thickness of 150 nm. With an increase in the rate of Ni deposition, the Ni contents increased from 61.5% to 69.6%. And, X-ray diffraction analysis verified that the films featured a face-centered cubic structure with variable peak intensities. Also, the scanning electron microscopy surface morphology analyses revealed that variations in the film surfaces were a result of the deposition rates. For magnetic measurements, the differences in the structural analysis were observed to cause a notable variation in saturation magnetization, M_S, and coercivity, H_C values. Accordingly, M_S values increased consistently between 359.0 and 389.7 emu cm^{-3}, but H_C values decreased from around 34–32 to 28 Oe with the increase in Ni deposition rate from 0.02 to 0.10 nm s^{-1}. It is also observed that when the Ni layers are generated at very fast deposition rates, the Ni/Al multilayer films have a high M_S/H_C ratio, which is significant for magnetic sensors. It has been concluded that the magnetisation of Ni/Al multilayer thin films can be controlled by the structural properties adjusting the Ni deposition rate.

1. Introduction

For many years, scientists have been interested in studying magnetic structures because of their potential applications in technology [1–8]. Research has frequently focused on examining the magnetic characteristics of the material and producing them with the needed features. Due to their high saturation magnetisation, M_S and low coercivity, H_C values, magnetically highly efficient materials are crucial parts of electromagnetic devices as magnetic isolators or in micro-electromechanical sensors and magnetic random-access memories [9–12]. The sputtering approach is one of several methods utilised to produce these kinds of nanoscale magnetic structures [12–14]. This method can be used to deposit high-quality thin films with the required characteristics. By adjusting the fabrication settings, the sputtering technique allows one to modify the physical properties of the films, including their magnetic properties. The deposition rate is one of the elements influencing the structure of the films in this context [13–15]. The effects of various Ni layer thicknesses and Al layer thicknesses on the magnetic characteristics of Ni/Al multilayer films were examined and the findings were described in detail in the studies by Karpuz *et al* [16] and Kaplan *et al* [17], respectively. As far as we are aware, no research has been done to examine how the various deposition rates influence the magnetisation of Ni/Al multilayer thin films, which are crucial for magnetic sensors and whose structural characteristics regulate magnetisation. The outcome of this study is anticipated to address this shortcoming and significantly advance the field of magnetic sensor applications and literature.

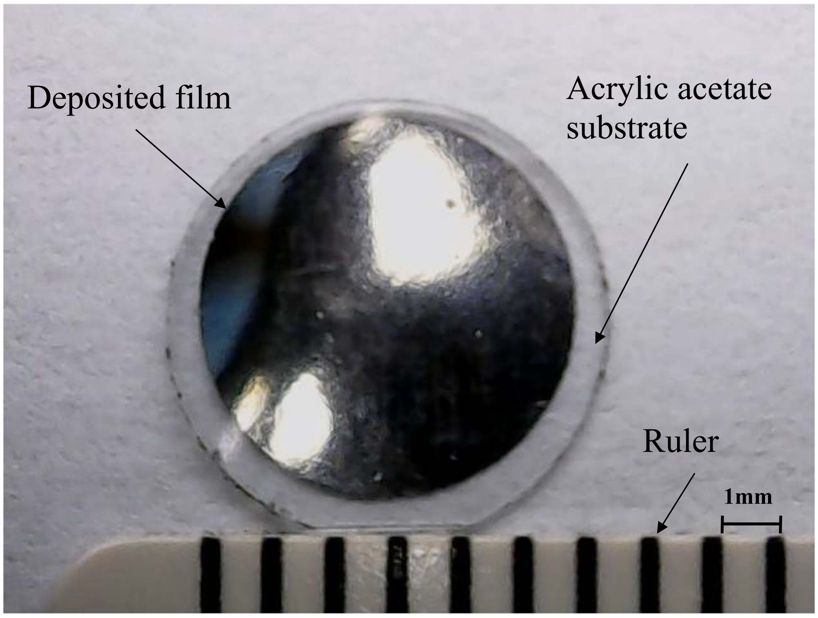

Figure 1. As deposited film sample with the ruler.

2. Experimental

Ni/Al multilayer thin films were deposited on flexible polymer substrates (0.168 ± 0.006 mm thick, Jeje Products, Acrylic Acetate Clear Sheets, Spain) by sputtering technique (MANTIS, Q-Prep 500, UK). This system also has features that allow the deposition rate of each layer to be controlled. Before starting the fabrication of the films, high-purity nickel and aluminium targets (Kurt J. Lesker Company, 99.99%) with a thickness of 2 mm and a diameter of 50.8 mm were first cleaned with distilled water followed by isopropyl alcohol in an ultrasonic bath (Isolab, 621.05.006, Germany) for 10 min each. The substrates were also prepared as the way the target was done. And, the average surface roughness value was around 30 nm as given by the manufacturer. The five substrates were cut by punching (6 mm in diameter) and used for sample fabrication. After cleaning, the targets and the substrate were placed in the vacuum chamber. The distance between the substrate and target sources in the vacuum chamber was 125 mm. For deposition, the pressure was first reduced to below 6.00×10^{-3} mBar using a rotary vane pump. A turbo molecular pump was used until chamber pressure dropped to 5.00×10^{-6} mBar to obtain a suitable vacuum environment for the fabrication and pure argon gas was introduced into the chamber for plasma creation. The argon gas flow rate was 60 sccm. The deposition of the films was carried out at a pressure range of approximately $4–5 \times 10^{-3}$ mBar. The substrate temperature was measured as 23 ± 3 °C during fabrication. The substrate was rotated (20 rpm) throughout the sputtering process to obtain more uniform films in terms of thickness. The rotational speed was measured using a handmade tachometer with an accuracy of $\pm$ 0.1 rpm. Film thicknesses were determined using a quartz crystal microbalance (QCM) thickness sensor connected to a thickness monitor (Sycon, STM-100/MF, US). After their fabrication, all films were stored in vacuum desiccators until analysis. Figure 1 shows an image of the deposited film.

To investigate the effects of deposition rate on the structural and magnetic properties of Ni/Al multilayer thin films, the Ni deposition rate was systematically varied from 0.02 to 0.10 nm s^{-1} in steps of 0.02 nm s^{-1}. Different deposition rates for Ni layers were adjusted by changing the electrical current value that occurred in the vacuum chamber. The electrical current values needed for different deposition rates of Ni layers and Al layers were added to table 1. The time between each one was around 60 s. The QCM thickness monitor also helped to observe the deposition rate values. Al deposition rate was kept constant at 0.02 nm s^{-1} in the fabrication of all films. Films with 5[Ni(20 nm)/Al(10 nm)] structures are illustrated in figure 2. A bilayer structure was formulated as [Ni(20 nm)/Al(10 nm)]. To obtain multilayer structure, the bilayer was repeated five times to obtain total film thickness of 150 nm. In other words, the number 5 is the number of repetitions of bilayer.

Content analyses of Ni/Al multilayer films were carried out using an Energy-dispersive X-ray Spectroscopy (EDX, EDAX Element, AMETEK, USA). The crystal structure of the films was detected using an X-ray Diffractometer (Bruker, Advance with Davinci Design for XRD^2, UK) with a LYNXEYE XE x-ray detector. Diffraction patterns of the films were obtained by the X-ray Diffraction (XRD) method using Cu-Kα radiation ($\lambda = 0.154059$ nm). Diffraction patterns were obtained between 30° and 80° by scanning the 2θ Bragg angle in 0.02° steps. The surface morphologies of the films were observed using a scanning electron microscope (SEM;

Table 1. Electrical currents, atomic contents, calculated crystal structure parameters and magnetic property values of the sputtered Ni/Al films at different Ni deposition rates.

Deposition rates (nm/s)		Electrical currents (mA)		Contents[a]		Crystal parameters		Magnetic values				
Ni	Al	Ni	Al	Ni (at. %)	Al (at. %)	a (nm)	t (nm)	M_S (emu/cm^3)	H_C (Oe)	M_S/H_C	M_r (emu/cm^3)	M_r/M_S
0.02	47	61.5	38.3	0.4084	9.1	359.0	32	11.18	228.3	0.636		
0.04		82		—	—	0.4080	9.2	371.4	34	10.92	262.3	0.706
0.06	0.02	112	216	65.5	34.3	0.4075	9.3	375.1	30	12.42	191.0	0.509
0.08		165		—	—	0.4067	9.5	387.9	28	13.89	143.2	0.369
0.10		217		69.6	30.2	0.4063	9.6	389.7	28	14.43	128.8	0.331

[a] All films contained up to 0.2 % of impurities such as H, O and C.

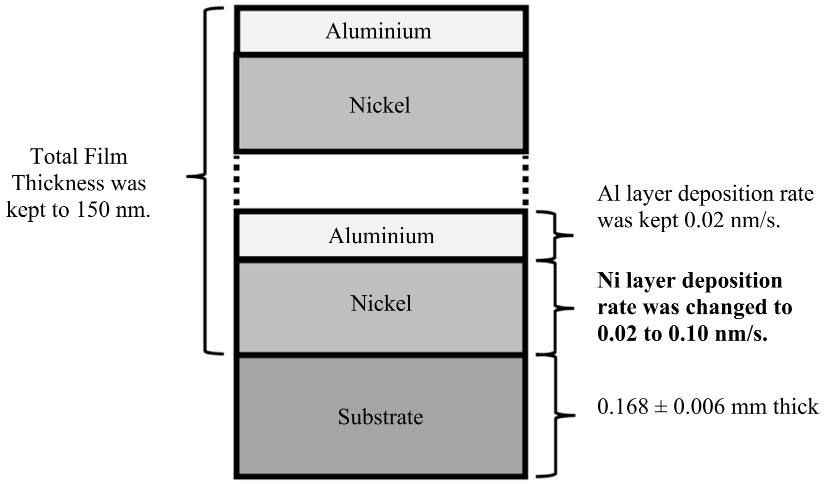

Figure 2. Schematic cross-section of the Ni/Al multilayer thin film structure.

Hitachi, SU5000, Japan). Magnetic analyses of multilayer films were carried out at room temperature using a vibrating sample magnetometer (VSM; ADE TECHNOLOGIES DMS-EV9, USA). Magnetic moments measured from VSM are divided by the calculated volume of the films to find the magnetisation values of hysteresis loops. Hysteresis loops were obtained at intervals (the smallest one is 1 Oe) between $\pm$ 20 kOe. The magnetic measurement sensitivity of the magnetometer was 1×10^{-6} emu. For the magnetic measurement process, the samples were cut into circles with a diameter of 6 mm to avoid shape anisotropy, see figure 1.

3. Results and discussion

3.1. Contents of the films

The analysis results of Ni/Al multilayer thin films obtained by EDX are presented in table 1. Content analysis shows that films with Ni deposition rates of 0.02, 0.06, and 0.10 nm s^{-1} consist of 61.5, 65.5, and 69.6% Ni atoms, respectively. Except for 0.2% consisting of Oxygen, Hydrogen and Carbon atoms coming from the substrate, the rest of the film contents were determined to be Al. According to the results, the Ni contents in the films increased with the increase in Ni deposition rate. The contents of the films show the same trend as the content ratios obtained in the study [16], in which the effects of different layer thicknesses of Ni layers for Ni/Al multilayer films were investigated.

3.2. Crystal structures of the films

Figure 3 shows the XRD patterns of Ni/Al multilayer thin films produced at different Ni deposition rates. In addition, no peak was observed in the pattern of the substrate due to its amorphous structure and therefore it was not shown in the figure. As seen in the XRD patterns, some differences in the peak intensities of the diffraction patterns were observed by changing the Ni deposition rate. The XRD patterns of the Ni/Al multilayer thin films have (111) peak of fcc Ni at $2\theta \approx 44.7°$ and (111), (200), (220) and (311) peaks of Al at $2\theta \approx 38.4°$, $44.7°$, $64.9°$ and $78.2°$ according to the JCPDS 88-2326 for Ni and JCPDS 04-0787 for Al, respectively. As seen in figure 3, with the increase in Ni deposition rate, the peak of the (111) plane of the face-centred cubic (fcc) Al, which is formed at Bragg angle of ~38.4°. The intensity of peaks in an XRD pattern is related to the atoms in the crystal lattice such as atomic number [18]. The higher intensity of the Al peak might come from depending on its atomic element number which is smaller than Ni. The peak numbered as 1 was almost the same while that of the peak formed at ~44.7° which is numbered as 2 and labelled as Al (200) + Ni (111) increases gradually. This increase in the intensity can be attributed to the increase in the Ni content of the film. Unlike the presented study, no peak at the angle of ~38° was observed in the XRD pattern of NiAl alloy films investigated in [19]. This may be because the investigated films have a multilayered structure or different substrates used in the presented study. Moreover, it has been determined that the peaks seen ~64.9° and ~78.2° belong to the Al fcc (220) and Al fcc (311) planes, respectively, and the intensities of these peaks decrease with the increase of Ni deposition rate. This change is consistent with the result obtained from the analysis of the film content. According to the crystal structure analysis, it was understood that all films crystallized in the fcc structure. The same peaks with the present study were also detected in the XRD pattern of as-deposited Ni/Al multilayer thin film with bilayer thickness of 30 nm in which a study [15] that investigated anisothermal solid-state reactions of Ni/Al.

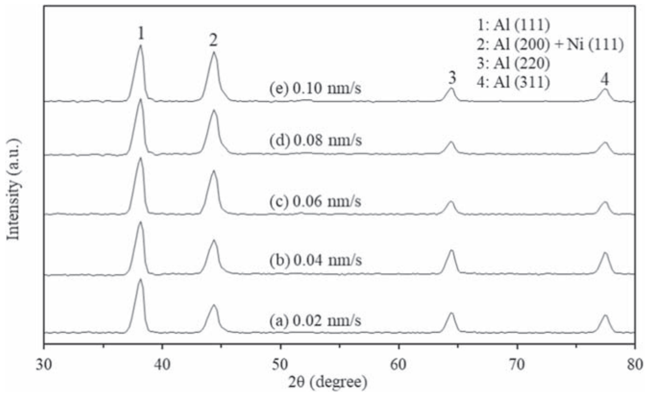

Figure 3. The XRD patterns of the films produced with different deposition rates of Ni layers (a) 0.02, (b) 0.04, (c) 0.06, (d) 0.08 and (c) 0.10 nm s^{-1}.

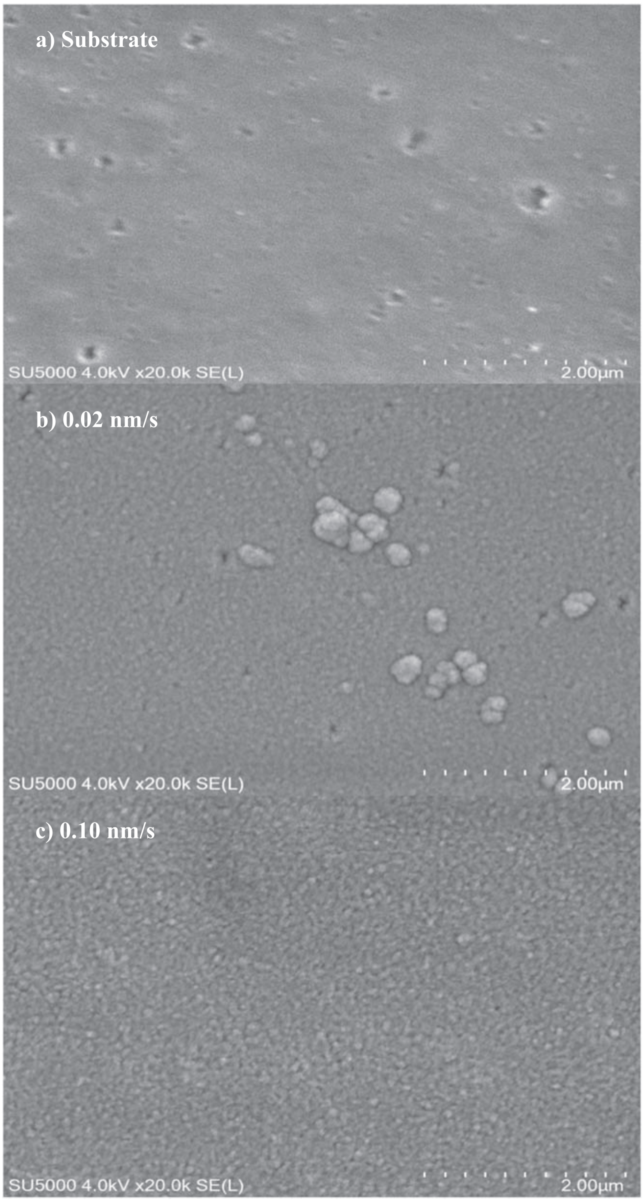

Figure 4. SEM images of (a) substrate and the multilayers sputtered with different Ni deposition rates at (b) 0.02 and (c) 0.10 nm s^{-1}.

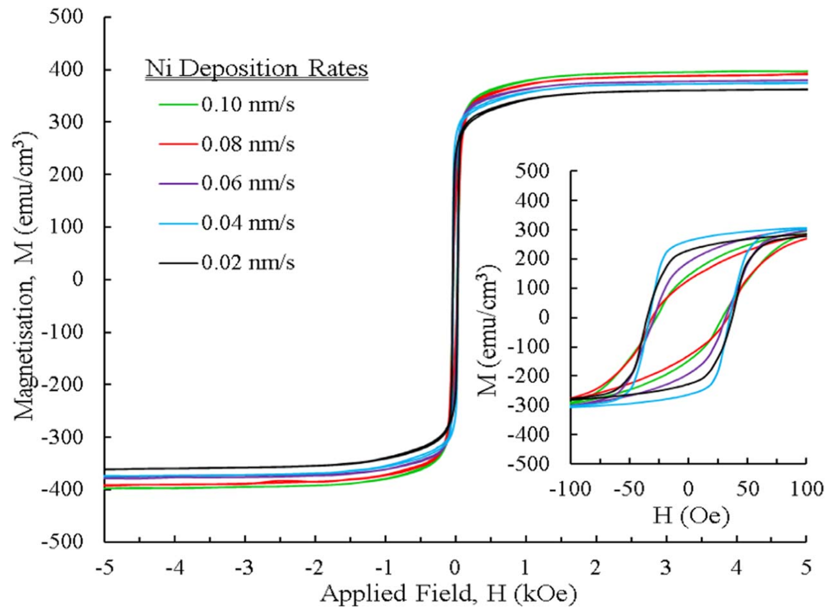

Figure 5. The hysteresis loops of the films produced with different Ni deposition rates between ±5 kOe magnetic field and inset between ±100 Oe magnetic field.

The crystallite sizes (given as t in table 1) of the films were calculated using the Scherrer equation as given in [18]. The crystallite sizes of Ni/Al multilayer films deposited at Ni deposition rates of 0.02, 0.04, 0.06, 0.08 and 0.10 nm s^{-1} were found to be 9.1, 9.2, 9.3, 9.5 and 9.6 nm, respectively. In addition, lattice constant (a) values were also calculated and found to be 0.4084, 0.4080, 0.4075, 0.4067 and 0.4063 nm for the films with Ni deposition rates of 0.02, 0.04, 0.06, 0.08 and 0.10 nm s^{-1}, respectively. In other words, the decrease in the content of Al resulting from the increase in the Ni deposition rate also caused a decrease in the lattice constant values.

3.3. Morphologies of the films

Figure 4 shows the SEM images of (a) substrate and Ni/Al multilayers (b) at the lowest (c) the highest Ni deposition rates. As seen in figure 4(a), although the substrate has some small defects, the films in figures 4(b)–(c)) are properly deposited. While there are some grain structures and dark points on the film surface produced with a low deposition rate, these structures are not available on the film surface sputtered at the high deposition rate. The sizes of these grains, randomly distributed on the surface, varied between 0.2 μm and 0.4 μm. Point measurements of EDX taken on these grains revealed that the surface grains have the same content as the rest of the film surface. When the films were produced with a high deposition rate, the surface had a relatively simpler and uniform appearance. Considering the relatively higher deposition rate, it is understood that better-quality film surfaces are obtained. As can be seen from the SEM images, the change in Ni deposition rates resulted in some differences in the morphologies of the film surfaces.

3.4. Magnetic properties of the films

For magnetic analysis, hysteresis loops of Ni/Al multilayer thin films sputtered at different Ni deposition rates are plotted in figure 5 ±5 kOe and inset ±100 Oe. Saturation magnetisation, M_S values of the films with Ni deposition rates of 0.02, 0.04, 0.06, 0.08 and 0.10 nm s^{-1} were detected to be 359.0, 371.4, 375.1, 387.9 and 389.7 emu cm^{-3}, respectively. It was observed that the M_S values of the films increased by increasing the Ni deposition rate (see figure 5 and table 1). In other words, the increase in the Ni deposition rate causes the density of the Ni layer of the films to increase, thus increasing the M_S values of the films. Coercivity, H_C values of films according to different deposition rates are given in table 1. When the table is examined, it is seen that H_C values tend to decrease between 34 Oe and 28 Oe with the increase of Ni deposition rate. The decrease in the H_C values of the films can be associated with the decrease in the amount of Al in the film content and, simpler and uniform surface morphologies with the increase in the Ni deposition rate. There are no studies about the magnetic properties of Ni/Al multilayer thin films except for our previous two investigations [16, 17]. The saturation magnetisation and coercivity values under study are found to be consistent with these studies. It was found that the film deposited with a Ni deposition rate of 0.10 nm/s had the highest M_S and lowest H_C values.

As displayed in table 1, M_S/H_C ratios of the films were also calculated and this ratio was found to be 11.18, 10.92, 12.42, 13.89 and 14.43 for films produced with Ni deposition rates of 0.02, 0.04, 0.06, 0.08 and 0.10 nm s^{-1}, respectively. As can be clearly seen, the highest M_S/H_C ratio was obtained in the film where the Ni deposition rate was 0.10 nm s^{-1}. In our previous study [16], it was emphasized that the M_S/H_C ratio increased by decreasing the Ni layer thickness and concluded that obtaining Ni/Al multilayer films with a high M_S/H_C ratio could be achieved with relatively low thickness values. The remanent magnetisation, M_r values determined for Ni/Al multilayer films with Ni layer deposition rates of 0.02, 0.04, 0.06, 0.08 and 0.10 nm s^{-1} were found to be 228.3, 262.3, 191.0, 143.2 and 128.8 emu cm^{-3}, respectively (see table 1). As shown in table 1, magnetic squareness (M_r/M_S) values were also calculated for the films. The values are 0.636, 0.706, 0.509, 0.369 and 0.331 for the films produced at 0.02, 0.04, 0.06, 0.08 and 0.10 nm s^{-1}, respectively. Although the magnetic squareness values increased as the Ni deposition rate increased from 0.02 to 0.04 nm s^{-1}, they gradually decreased for further rate values. The same trend was also observed for the M_r values. Since the M_r value is an independent parameter [12], changes in crystallite sizes and film surface morphology may be the reason for the change in M_r/M_S values.

4. Conclusions

Within the scope of this study, the dependence of macroscopic magnetic behaviour controlled by structural properties was investigated, which are affected by the deposition rate of Ni layers in Ni/Al multilayer thin films. For this purpose, using the sputtering process, a series of 150 nm thick 5[Ni(20 nm)/Al(10 nm)] films were deposited on acrylic acetate substrates. The findings showed that as the Ni layer deposition rates increased from 0.02 to 0.10 nm s^{-1}, the Ni contents of the films increased from 61.5% to 69.6%. All of the films have a face-centred cubic structure, as validated by structural analysis. And, the results of surface research indicated that the creation of more favourable and moderate film surfaces was facilitated by relatively high deposition rates. The microstructural alterations on the film surface and the variation in the concentration of Al in the multilayers were identified as the causes of the H_C change. It was found that changes in surface shape and film contents brought about by variations in the rate of deposition resulted in changes in magnetic characteristics like M_S and H_C, which are significant for sensor applications.

Acknowledgments

Authors are grateful to Balikesir University BAP under grant no 2022/068 for the financial funding. This study was also funded by the State Planning Organization/Turkiye under grant no 2005K120170 for physical vapour deposition system and VSM systems. Authors also thank the Karamanoğlu Mehmetbey University, BILTEM, Turkiye for XRD, SEM and EDX measurements. Nadir Kaplan privately acknowledges The Scientific and Technological Research Council of Turkiye (TUBITAK), 2211-C National Scholarship Program for Ph.D study.

Data availability statement

The data cannot be made publicly available upon publication because they are not available in a format that is sufficiently accessible or reusable by other researchers. The data that support the findings of this study are available upon reasonable request from the authors.

Fundings

Authors are grateful to Balikesir University BAP under grant no 2022/068 for the financial funding. This study was also funded by the State Planning Organization/Turkiye under grant no 2005K120170 for physical vapour deposition and VSM systems. Nadir Kaplan privately acknowledges The Scientific and Technological Research Council of Turkiye (TUBITAK), 2211-C National Scholarship Program for Ph.D study.

Declarations

The data that support the findings of this study are available upon request from the authors.

Author contributions

Nadir Kaplan produced the films according to the experimental plan and prepared the table and figures, and also wrote the draft of the article. Ali Karpuz helped to take and interpret the XRD, SEM and EDX measurements and also wrote the article. Hakan Köçkar planned and directed the study and contributed to the measurements and interpretation of all results.

Conflict of interest

The authors declare that they have no conflict of interest.

ORCID iDs

Nadir Kaplan https://orcid.org/0000-0002-2471-1179
Ali Karpuz https://orcid.org/0000-0002-3050-1549
Hakan Köçkar https://orcid.org/0000-0002-4862-0490

References

[1] Sahu D R 2024 Magnetic nanostructures for transport control and sensing applications *Nanoscale Matter and Principles for Sensing and Labeling Applications. Advanced Structured Materials* ed D Mohanta and P Chakraborty (Springer) 206 (https://doi.org/10.1007/978-981-99-7848-9_28)
[2] Shirsat S D, Londhe P V, Gaikwad A P, Rizwan M, Laha S S, Khot V M and Thorat N D 2024 Endosomal escape in magnetic nanostructures: Recent advances and future perspectives *Materials Today Advances* **22** 100484
[3] Li J, Li G, Lu X, Wang S, Leng M, Yang S and Long Y 2024 Magnetically responsive optical modulation: from anisotropic nanostructures to emerging applications *Adv. Funct. Mater.* **34** 2308293
[4] Yin Y 2024 Photothermal and magnetic heating of nanostructures for biomedical applications *Colloidal Nanoparticles for Biomedical Applications XIX* PC1285909(SPIE)
[5] Elsafi B 2024 Contribution of surface scattering to the GMR effect in the magnetic multilayer films *Indian J. Phys.* 1–6
[6] Tang Y, Xu X, Yang J, Ren L, Cao H, Zhao N and Ouyang X 2024 Effect of negative bias voltage on microstructure and thermal stability of Cu/Nb nano-multilayers deposited by FCVA technique *Mater. Charact.* **210** 113851
[7] Liu S, Kästner P, Donatiello R, Shrivastava A, Smolarczyk M, Iskhandar M S Q and Hillmer H 2024 State-of-the-art materials used in MEMS micromirror arrays for photonic applications *Photonics, MDPI* **11** 253
[8] Torkashvand Z, Shayeganfar F and Ramazani A 2024 Nanomaterials based MicroNanoelectromechanical system (MEMS and NEMS) devices *Micromachines* **15** 175
[9] Wang Z, Zhang M, Yang K, Yu T, Lv B, Chen Y and Wang X 2024 Coupling of magnetic field noise in multilayer magnetic shields for atomic magnetometer *IEEE Trans. Instrum. Meas.* **73** 3353834
[10] Chen C, Pan P, Gu J, Liu M and Li X 2024 Design and wafer-level fabrication of stacked-type transformers for high-density power converters *IEEE Trans. Power Electron.* **39** 4503–12
[11] Talapatra A, Weisheit M, Müller J, Mansueto M, Hazen D S, Komma V S and Zaka A 2024 Modeling methodology for thermal stability factor in spin transfer torque magneto-resistive random access memories *IEEE Trans. Electron Devices* **71** 1886–92
[12] Brück E H 2017 *Handbook of Magnetic Materials* (Elsevier)
[13] Nimalan T and Begam M R 2024 Physical and chemical methods: a review on the analysis of deposition parameters of thin film preparation methods *Int. J. Thin. Fil. Sci. Tec.* **13** 59–66
[14] Seshan K and Schepis D (ed) 2018 *Handbook of Thin Film Deposition* (William Andrew)
[15] Simões S, Viana F, Ramos A S, Vieira M T and Vieira M F 2011 Anisothermal solid-state reactions of Ni/Al nanometric multilayers *Intermetallics* **19** 350–6
[16] Karpuz A, Köçkar H and Çölmekçi S 2018 Structural and corresponding magnetic properties of sputtered Ni/Al multilayer films: effect of Ni layer thickness *Acta Phys. Pol. A* **134** 1180–6
[17] Kaplan N, Kuru H and Köçkar H 2024 Investigation of the influence of Al layer and total film thicknesses on structural and related magnetic properties in sputtered Ni/Al multilayer thin films *J. Mater. Sci., Mater. Electron.* **35** 1–9
[18] Cullity B D 2014 Elements of x-ray diffraction 3rd edn (Pearson New International Edition)
[19] Mahesh R A, Jayaganthan R, Prakasha S, Vipin C and Ramesh C 2009 High temperature cyclic oxidation behavior of magnetron sputtered Ni–Al thin films on Niand Fe-based superalloys *Mater. Chem. Phys.* **114** 629–35